

# Urban Vegetation Change Detection based on Image Information Enhancement

**Hao He\*, Xinyu Liao, Xinling Hu, Shijun Lu, Haibin Shang**

College of civil and architectural engineering, Xinjiang University, Urumqi, 830017, China

\*Corresponding Author.

## **Abstract:**

In this paper, a kind of urban vegetation change detection method based on image information enhancement is proposed for the problem of error detection caused by the haze and shadow in vegetation change detection of urban high-resolution remote sensing images. Firstly, conduct haze removal on images through HSV transformation; then, carry on vegetation shadow compensation by PESR method; next, perform the vegetation information post-processing by using SNDS method; finally, obtain the information on vegetation change by using difference method. The vegetation change detection on WorldView-2 image and Ikonos image of Xi'an City shows that the average precision reaches 80.81%. The experimental results indicate that the proposed method in this paper has brought about a certain improvement of vegetation identification rate in the high-resolution image and a significant decrease in missing extraction of vegetation information in shadow area, thus effectively improving the accuracy of vegetation change detection.

**Keywords:** *Image information enhancement, high-resolution remote sensing, vegetation, change detection.*

---

## I. INTRODUCTION

How to conduct the effective, accurate and automated identification and detection on changes of green vegetation as the important ground objects is one of the hot issues in the application of remote sensing<sup>[1]</sup>. For the occlusion and shadow in large areas produced by the more and more high-rise buildings in modern cities, the influence of buildings leads to the strong changes in the spectral characteristics of vegetation in occlusion area and shadow, thus making the same vegetation category have different spectral characteristics in different scenes. The usually missing identification on vegetation in shadow area and the occasionally mistaking of shadow to be vegetation confirm that the existence of haze and shadow makes it difficult for the automated identification and change detection on vegetation due to the significant increase in the uncertainty of vegetation spectrum.

The band ratio and vegetation index have been widely used in vegetation shadow removal. For example, the ability of NDVI to greatly reduce the influence of illumination condition changes and shadow effect caused by changes in sunlight and viewing angle<sup>[2]</sup> is served as the basis for the generation of various methods for shadow removal. The topological correction method adopted by Riano et al.<sup>[3]</sup> for the correction on vegetation shadow areas in Landsat TM images reduces the distortion of vegetation spectral information in images and the standard deviation of each vegetation type. Aiming at the problem of big error in image classification caused by the uneven reflectivity of shadow area, Yesilnacar et al.<sup>[4]</sup> reduce the impact of shadow on image classification by referring to the information on vegetation, forestry, etc. Matsushita et al.<sup>[5]</sup> take the airborne images of two artificial cypress forests with high density as objects to study the performance of normalized vegetation index and enhanced vegetation index in vegetation shadow areas, with the results showing that the more sensitivity of enhanced vegetation index to shadow requires the adoption of parameter modification method to remove the shadow and the impact of rough terrain on index results. A shadow removal method integrating photochemical reflectance index (PRI) and red-edge normalized difference vegetation index (RENDVI) proposed by Xiaolong Liu et al.<sup>[6]</sup> is to carry on the removal through the separation of shadow from vegetation and non-vegetation regions by setting PRI and RENDVI as threshold for shadow detection. At the same time, a new method proposed by Jiang Hong et al.<sup>[7]</sup> to eliminate the impact of shadow on vegetation index can obtain the shadow elimination vegetation index SEVI by using ratio vegetation index RVI, shadow vegetation index SVI and adjustment factor  $f(\Delta)$ . An image shadow removal method based on sub-region matching light transmission is proposed by Chunxia Xiao et al.<sup>[8]</sup>, which firstly carries on shadow detection and segmentation by referring to the shadow characteristics inside HIS space, and then performs illumination transfer on the matching sub-regional pairs between the shadow area and the non shadow area, so as to realize the shadow removal of images.

The shadow compensation method in the early stage based on the performing of overall compensation through the linear relationship between the mean value, mean square deviation of shadow region and those of non shadow region<sup>[9]</sup> is only appropriate for shadow repair in the homogeneous areas of large woodlands, which will make the phenomenon of over-compensation or under-compensation happened to the urban regions with high heterogeneity. According to the principle of "proximity is similarity" as the first law of geography, the method of taking the non shadow area within the certain range around shadow as the compensation reference region to carry on shadow repair with the great improvement in repair effect is effective in most cases, but is still inapplicable in complex and changeable urban areas. In the case of the adjacency of various ground objects, such as the vegetation in the shadow of buildings, the non shadow area around the shadow with vegetation and buildings, the correction mistake will be inevitably happened when directly taking all the non shadow areas within certain range around the shadow as the reference for compensation.

Aiming at the above problem, the high-resolution true color remote sensing images are used in this paper to carry on the research from the aspects of image information enhancement and "salt-pepper" noise removal. The improvement for the unreasonable selection of shadow reference region in the current vegetation shadow repair method has promoted the proposal of parallel-edge shadow repair method (PESR). For the insufficient utilization of spatial information in the extracted vegetation information, the vegetation spatial neighborhood density segmentation method (SNDS) is proposed to conduct further processing on the extracted information by adding spatial information to reduce the "pepper and salt" noise. The overall research idea of this paper is shown in Fig 1.

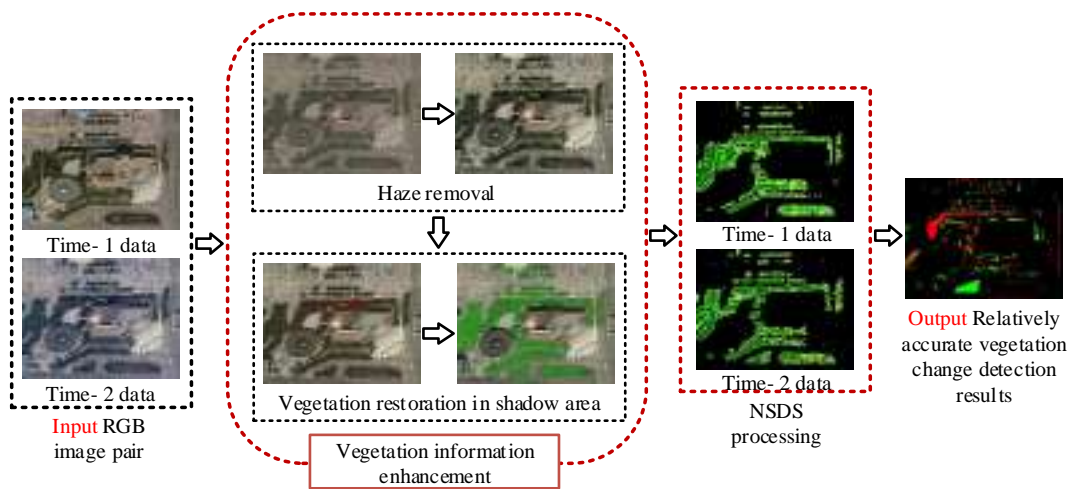


Fig 1: Overall Research Idea of This Paper

## II. METHODS

### 2.1 Haze Removal Based on HSV Transformation

Under the influence of urban dust-haze on color remote sensing image, the reduction of image saturation (S) and the increase of image brightness value (V)<sup>[10]</sup> promote the adoption of the way of stretching the components S and V to conduct enhancement on remote sensing images to improve the separability of urban vegetation<sup>[11]</sup>, whose specific steps are as follows: Firstly, switch the original RGB image to HSV (Hue,Saturation,Value) color space; secondly, after taking the 1% of the minimum and maximum values in component S to be respectively set as 0 and 1, conduct linear stretching on residual pixels to form the enhanced component S\_en; meanwhile, the enhanced component V\_en of component V is obtained in the similar way; thirdly, the replacement of components S and V respectively by S\_en and V\_en forms the enhanced HSV image to be marked as HSV\_en; fourthly, perform the inverse transformation on HSV\_en to make it converted into RGB image, so as to form the enhanced image RGB\_en.

Fig 2 (a) and Fig 2 (b) as the images before and after enhancement show the ability of enhancement to highlight the differences between flora and other features and improve the integrity of crown contour.



Fig 2: Haze Removal based on HSV transformation

### 2.2 Vegetation Shadow Compensation Based on PESR

With the focus on optimization and improvement for the selection of shadow compensation reference region in the method of this research, the parallel lines are respectively drawn on the inside and outside of shadow boundary line, so as to conduct correlation analysis on the brightness values of the pixels where the inner and outer parallel lines in a certain range are located. Then, set the threshold to eliminate the sections with low correlation, and reserve the sections with high correlation as the compensation reference region. Carry on the compensation calculation by taking shadow pattern patches as unit. As shown in Fig 3, the red lines are the shadow boundary lines, while the blue and green lines are the inner and outer parallel lines of shadow boundary lines, respectively.



Fig 3: Selection of Shadow Compensation Reference Region

As shown in Fig 3, with the realizable extraction of inner and outer double parallel lines in the large areas of shadow area (red lines and blue lines), the inner parallel lines degenerate into points or even disappear in the small areas of shadow area. The small shadow areas in the figure are mostly the crown shadow, whose surroundings are trees, vegetation and other ground objects in the same category, while the large shadow areas are mostly the falling shadow area of tall buildings, which are surrounded by a variety of ground objects.

### 2.3 Vegetation Information Post-processing Based on SNDS

In the remote sensing image classification, the frequent adoption of spatial position relation of target ground object as the supplement to spectral characteristics for the improvement of classification effect has pushed the emergence of a series of geographical location weight methods based on spectral-spatial joint analysis<sup>[12, 13]</sup>, such as geographical location weighted regression<sup>[12]</sup>, etc., in which, the neighborhood density function of image target ground object members (pixels or image patches) can provide a meaningful reference for image analysis. For example, two categories of discretely distributed ground objects can be distinguished according to the difference of neighborhood density values in a specific spectral feature space, even if they are mixed with each other in the feature space, without obvious feature dividing line / face. In addition, with the ability of reflecting the probability that a pixel belongs to this kind of ground object in a certain area to some extent, the spatial neighborhood density value can be also called spatial neighborhood distribution probability, which is the extension of spectral-spatial joint analysis. The spatial neighborhood density segmentation of vegetation distribution in this paper is based on the following two assumptions: The first is that the appropriately designed spatial distribution probability variable can represent the spatial context relationship between target ground objects; the second is that introduce this variable into the analysis results of spectral characteristics to enhance the spatial context attribute of analysis results, thereby improving the ability to distinguish urban vegetation from other ground objects.

The influence of spectrum noise makes the vegetation information extracted by directly using RGB color remote sensing images show the scattered distribution in geographical space, thus the usual failing of forming meaningful pattern patches requires the further processing on it. In the experiment of remote sensing image segmentation or classification, it is easy to find the rule that the pixel (pattern patch) density of relatively certain target ground object is high in geographical space, while that of those uncertain target ground objects is low, thus indicating that the spatial neighborhood density can represent the degree of certainty of target ground objects.

$$D(i, j) = \text{count}(B_{w \times w}) / A \quad (1)$$

Where,  $D(i,j)$ =Spatial neighborhood density value of the row  $i$  and column  $j$ ;  $\text{count}(\cdot)$ =Counting function;  $B$ =Element of target ground object in the  $w \times w$  neighborhood with  $(i,j)$  as the center;  $A$ =Area of the current  $w \times w$  neighborhood.

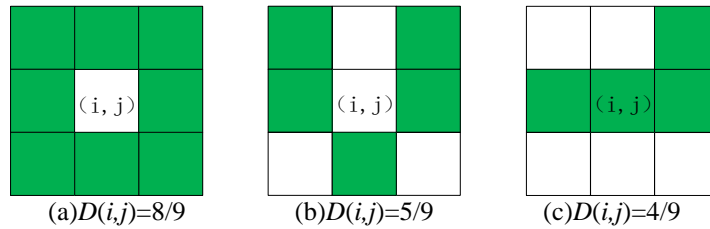


Fig 4: Diagrammatic Sketch for Vegetation Probability of Central Pixel

With vegetation as target ground object for calculation, the spatial neighborhood density value can be used to represent the probability that the pixel is vegetation. For example, when  $w=3$ , the probability that the central pixel is vegetation is shown in Fig 4, where the green pixel is the pixel determined as vegetation during preliminary extraction of vegetation.

The calculation on the initial vegetation extraction results according to the  $w \times w$  neighborhood helps to obtain the probability values that all the pixels belong to vegetation within their  $w \times w$  neighborhood, with the range of probability values of pixels belonging to vegetation as  $[0, 1]$ . Then, the vegetation probability values of all the pixels in the figure are conducted with automatic threshold segmentation by using Otsu method, and the pixels larger than the segmentation threshold are divided into several levels according to their probability values, which are expressed hierarchically. For example, conduct the vegetation spatial neighborhood density segmentation on the  $7 \times 7$  neighborhood, with the image comparison before and after processing shown in Fig 5.

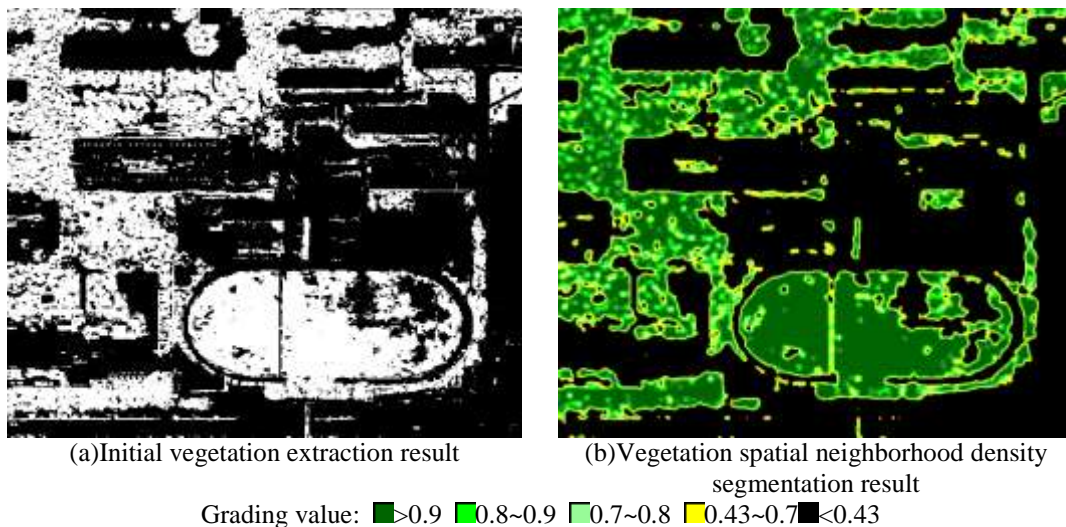


Fig 5: Comparison of Vegetation Spatial Neighborhood Density Segmentation

As shown in Fig 5, the "salt-pepper" noise generated by pixel method is significantly improved after the spatial neighborhood density segmentation, with the non vegetation noise effectively removed. However, due to the dependence of spatial neighborhood density segmentation processing effect on the precision of initial vegetation extraction, if there are many misidentifications in initial vegetation extraction, the correction on large area can not be realized only by spatial neighborhood density segmentation that is still a kind of filtering and denoising method essentially.

### III. EXPERIMENT

#### 3.1 Experimental Data

A place in the urban area of Xi'an was selected as the experimental area (shown in Fig 6). The Google Maps image and the Map World image downloaded by using Loca Space Viewer software are selected as remote sensing images. The front and rear time phase images are the remote sensing images spliced from RGB three-band 18-level tile data, with the spatial resolution of 0.6m, in which, the Map World image (shot in 2016) and the Google Maps image (shot in 2017) are respectively taken as time phase 1 and time phase 2. The two images both shot in summer with the basically same time phase have the clear imaging due to the inexistence of cloud coverage in the experimental area, thus being able to meet the requirements of urban vegetation change detection experiment.



Fig 6: Sketch Map of Experimental Area

Among the two sub experimental areas selected from the experimental area (Fig 7), the sub experimental area A belonging to the common urban vegetation scenes has not only the vegetation in shadow but also the blue-roof houses, with certain vegetation change area. The sub experimental area B

with vegetation area accounting for a high proportion can represent the major type of urban vegetation, including grassland, forest and shadow interference area. With the area B as the main source of vegetation extraction in the previous part, the area A will be conducted with vegetation extraction and change detection experiment in the next part.



Fig 7: Original Experimental Data

### 3.2 Vegetation Information Extraction Experiment

As shown in Fig 8, the vegetation without the performing of vegetation information enhancement extraction is compared with the vegetation extracted after enhancement to verify the vegetation extraction effect of vegetation information enhancement method in this paper, in which, figure (a) is the image obtained from the relative radiation correction on time phase 2 original image, figure (b) is the image of haze removal, figure (c) is the reference vegetation information, figure (d) is the result of directly conducting vegetation information extraction on original image, figure (e) is the vegetation information after vegetation restoration in the shadow area, and figure (f) is the result of vegetation information post-processing based on SNDS.

The comparison between Fig 8 (a) and Fig 8 (b) shows that the processing of haze removal on vegetation results in the clearer image and the more obvious vegetation boundary, so as to be more conducive to the accurate identification of vegetation information. The comparison of vegetation information extraction results between Fig 8 (d) and Fig 8 (e) shows the ability of vegetation restoration in shadow area to significantly reduce the misidentification on vegetation in shadow area. However, there are still many holes in the extracted vegetation information, while the holes and their surrounding noise information can be removed through SNDS processing (Fig 8 (f)).

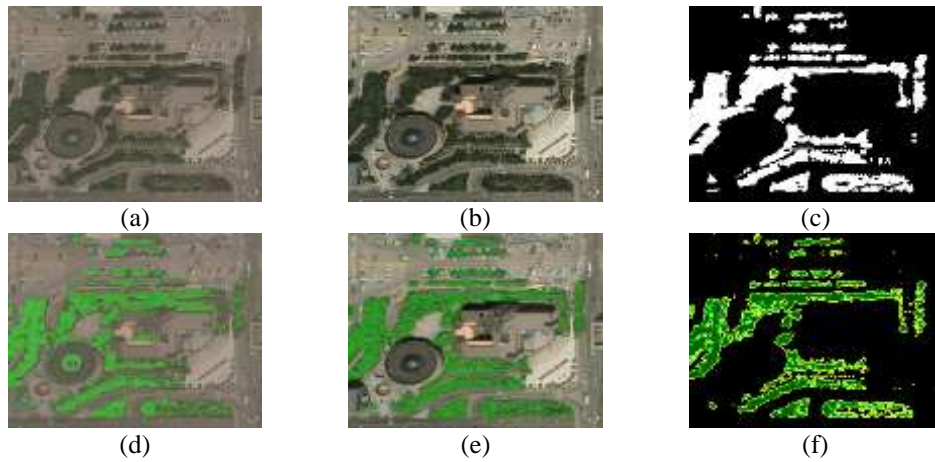


Fig 8: Comparison Before and After Vegetation Information Enhancement and Vegetation Information Extraction

In spatial neighborhood density segmentation (SNDS), the value of  $w \times w$  neighborhood of pixel also has a certain impact on vegetation extraction precision, so in order to determine the relationship between neighborhood scale and vegetation extraction precision under the resolution of this experimental data, the following experiment is carried out: Respectively set the neighborhood scale as  $w = \{3, 5, 7, 9, 11, 13\}$  to extract vegetation information, and then calculate the vegetation extraction precision of each scale to draw the line chart, as shown in Fig 9.

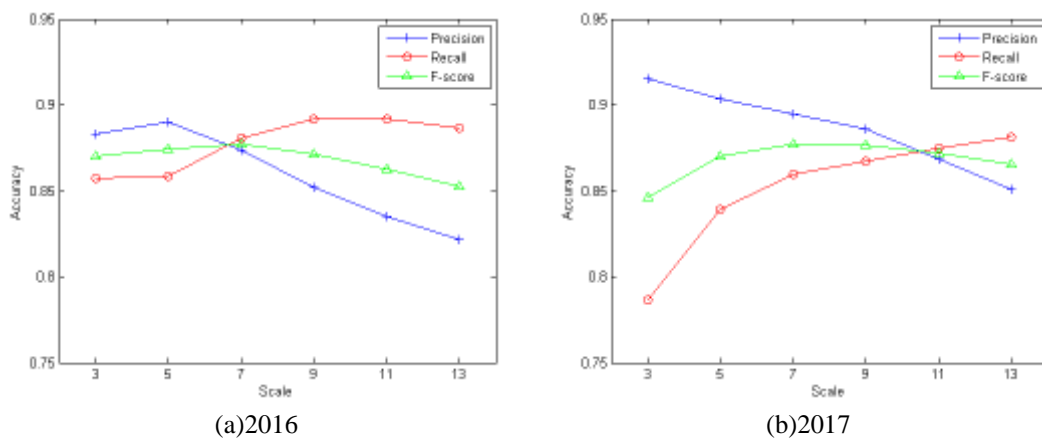


Fig 9: Sketch Map for the Relationship between Neighborhood Scale and Vegetation Extraction Precision

As shown in Fig 9, the experiment on the images of time phase 1 (2016) and time phase 2 (2017) in the experimental area A shows that the gradual increase in neighborhood scale pushes the precision, recall and weighted overall performance index to show a trend of rising first and then declining. The

various indexes of the two phase images in the overall reach to be optimal when the scale is taken as 7 and 9. Therefore, the scale is taken as 7 in this paper for the follow-up experiment.

The three methods used for the extraction and comparison of vegetation information in this paper are as follows: The first method is to directly extract vegetation from the original images of the two time phases by using NDSV index method; the second method is to extract the vegetation from the images performed with vegetation information enhancement by using NDSV index; the third method is to take the neighborhood scale as 7 to conduct spatial neighborhood density segmentation on the extraction result of vegetation information enhancement. According to the three commonly used indicators<sup>[14]</sup> in target recognition field, namely, precision, recall and weighted overall performance index ( $F_{\beta}$ -score), the vegetation precision extracted by the three methods is conducted with performance evaluation, as shown in Table I.

**TABLE I. Precision comparison of vegetation information extraction results**

Image	Vegetation extraction method	Precision(%)	Recall(%)	$F_{\beta}$ -score
Time phase 1	Method 1	78.80	78.58	0.7868
	Method 2	<b>88.91</b>	79.29	0.8383
	Method 3	87.39	<b>88.08</b>	<b>0.8773</b>
Time phase 2	Method 1	79.67	67.56	0.7311
	Method 2	<b>90.13</b>	77.39	0.8327
	Method 3	89.50	<b>85.97</b>	<b>0.8770</b>

As shown in Table I, compared with the way of direct vegetation information extraction from the original image, the way of vegetation information extraction after vegetation information enhancement shows significant improvement in precision, recall, weighted overall performance index ( $F_{\beta}$ -score) and other aspects. With the ability of bringing about further improvement in recall and weighted overall performance ( $F_{\beta}$ -score), the follow-up spatial neighborhood density segmentation processing makes the precision decrease a little, which is because that besides carrying on the non vegetation noise removal and hole filling in vegetation area, the SNDS processing can also be prone to misjudge the non vegetation pixels at the edge of some vegetation areas as vegetation, thus resulting in the small decrease in precision. In terms of weighted overall performance, SNDS has the best vegetation extraction performance.

### 3.3 Vegetation Change Detection Experiment

Based on the vegetation information of the two time phase images before and after vegetation information enhancement, the results of initial vegetation change detection obtained by difference method is conducted with further processing by SNDS, with the experimental results shown in Fig 10, in which, the comparison method 1 is the change detection result by the difference method of direct vegetation extraction, while the comparison method 2 is the change detection result by the difference method of vegetation information enhancement, and this paper adopts the way of combining the difference method of vegetation information enhancement with SNDS post-processing.

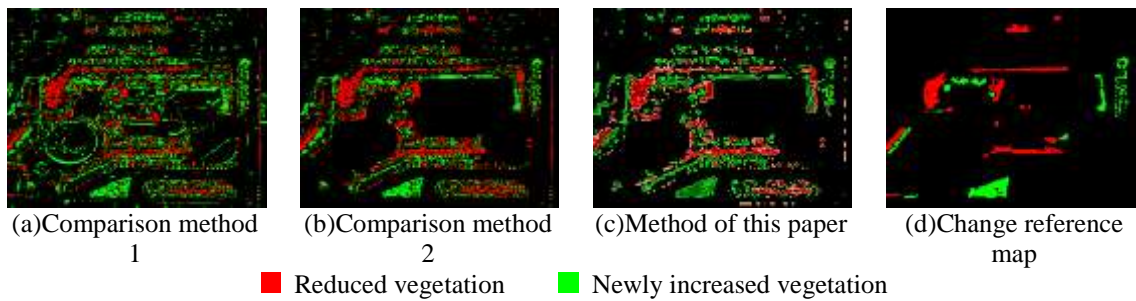


Fig 10: Visual comparison of vegetation change detection results

The detection results show that for the comparison method 1, the strong uncertainty of vegetation spectrum caused by the impact of haze and shadow brings about more vegetation misidentification and missing identification, thus the detection results have more noises as well as the obvious false detection and missed detection; for the comparison method 2, with the impact of shadow and haze eliminated by vegetation information enhancement processing, the relatively stable vegetation spectral information brings about the obvious improvement in detection results; for the proposed method in this paper, the removal of holes and noises realized by the further addition of post-processing on spatial information makes the detection results better. However, the impact of image parallax pushes the generation of certain deviation in the imaging position of trees above the ground on the image, thus resulting in more false detection and missed detection in the change detection of dual phase image difference method. In the overall, the proposed method in this paper can significantly improve the precision of vegetation change detection, which can be better verified by the good quantitative comparison results (Table II).

**TABLE II. Quantitative comparison of vegetation change detection results**

Change detection method	OA(%)	FA(%)	MA(%)	Kappa

Comparison method 1	63.28	41.13	35.80	0.4142
Comparison method 2	76.24	24.27	22.78	0.6836
The proposed method	<b>80.81</b>	<b>22.11</b>	<b>18.80</b>	<b>0.7045</b>

The quantitative error evaluation index of vegetation change detection results includes overall precision, false alarm rate, missed-detection rate<sup>[15]</sup> and Kappa coefficient<sup>[16]</sup>, in which, the overall accuracy (OA) refers to the ratio of the correctly detected changed pixel and the unchanged pixel to the total number of pixels; the false alarm rate (FA) refers to the proportion of unchanged pixels detected as changed pixels; the missed-detection rate (MA) refers to the proportion that the pixels actually change but are not detected as changed pixels.

#### IV. DISCUSSION AND ANALYSIS

In the comparison experiments designed for verifying the effect of the proposed method in vegetation change detection, the first group adopts the way of combining classic change detection method with NDSV vegetation information extraction to determine the vegetation changes; the second group adopts the way of combining classic change detection method with the proposed method in this paper to obtain the vegetation changes, with their results compared to verify the effectiveness of the proposed method through visual comparison and quantitative numerical comparison. The selected classic methods contain the pixel-based change detection method (Kittler and Illingworth's, KI)<sup>[17]</sup>, object based change detection algorithm (OBCD)<sup>[18]</sup>, spectral correlation mapping (SCM)<sup>[19]</sup> and spectral gradient difference method (SGD)<sup>[20]</sup>.

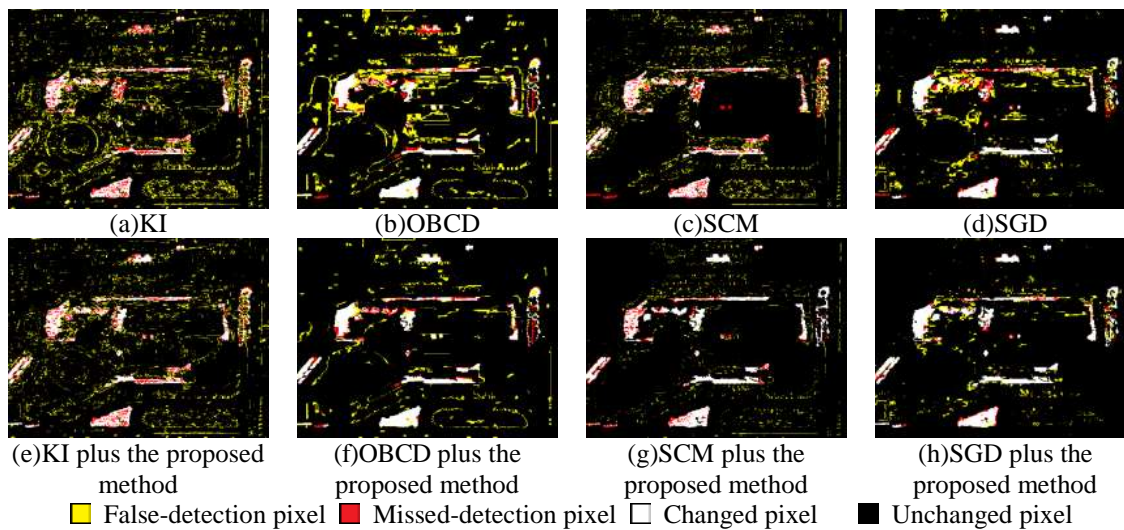


Fig 11: Vegetation Change Detection Results of Different Detection Techniques

In Fig 11, among the detection results of the four classic methods and those of their respective combinations with the proposed method in this paper, the colors of white, black, yellow and red respectively represent the changed pixel, the unchanged pixel, the false-detection pixel and the missed-detection pixel. The comparison of experimental results between the two groups shows that SCM and SGD have the best detection effect, while KI and OBCD have the obvious false detection and missed detection, and the experimental result of the second group is better than that of the first group, which also indicates that removing the shadow and the impact of haze can make the detection effect of various detection methods significantly improved. See Table III for the quantitative comparison data of detection results by different methods.

In order to quantitatively evaluate the detection results of various change detection methods, three error detection indexes including missed-detection error (MD), false-detection error (FA) and the overall error (OE) as well as a comprehensive evaluation index Kappa are selected in this paper to evaluate the detection methods from the aspects of error detection situation and the overall performance, in which, MD refers to the number of pixels that actually change but are not detected, FA refers to the number of pixels that have no change but are determined as the changed pixels, and OE the sum of the number of missed-detection and false-detection pixels.

Table III indicates the improvement of the combination of the proposed method and classic methods in detection performance from the quantitative perspective, shown in the great decrease of the overall error and the significant increase of Kappa coefficient. For example, the combination with the proposed method in this paper has made the Kappa coefficients of KI, OBCD, SCM and SGD respectively increased by 0.1648, 0.2260, 0.2405 and 0.1811.

**TABLE III. Quantitative comparison of vegetation change detection results of different detection techniques**

Change detection method	MD	FA	OE	Kappa
KI	6313	27682	33995	0.4381
KI plus the proposed method	5100	18134	23234	0.6029
OBCD	4665	25674	30339	0.5360
OBCD plus the proposed method	3542	10412	13954	0.7620
SCM	5919	14312	20231	0.6254

SCM plus the proposed method	3219	5492	8711	0.8659
SGD	4211	14386	18597	0.6793
SGD plus the proposed method	2196	7327	9523	0.8604

## V. CONCLUSIONS

In this paper, a kind of urban vegetation change detection method based on image information enhancement is proposed to study the removal of urban haze and shadow in high-resolution images. Carry on the haze removal through HSV transformation; the improvement for the unreasonable selection of reference region in the current shadow removal method pushes the proposal of parallel-edge shadow repair method (PESR) for spectral restoration of vegetation in shadow area; the spatial neighborhood density segmentation (SNDS) method is put forward to carry on the post-processing of the extracted vegetation information added with spatial information. The effectiveness of the proposed method in vegetation change detection is verified by experiments, with the main conclusions as follows:

(1) Adopt the way of stretching the components S and V to conduct enhancement on remote sensing images, so as to highlight the differences between flora and other ground objects and improve the integrity of crown contour.

(2) Relative to the direct vegetation information extraction without shadow compensation, the vegetation information extraction after shadow compensation have a certain improvement in identification rate and can bring about a significant reduction in missing extraction of vegetation information in shadow area. However, some dark shadow areas with very low reflectivity (the almost black shadow areas with weak light and shade changes in the image) has the insignificant effect of shadow compensation, whose performing of shadow repair fails to play a positive role in vegetation information extraction due to being prone to color distortion with the tendency to be blue or red. Therefore, the vegetation information restoration method in shadow area is only applicable to vegetation information enhancement in bright shadow area.

(3) In this paper, the proposed method of spatial neighborhood segmentation can effectively remove the "salt-pepper" noise in the extracted vegetation information, and for the experimental image in this paper, the optimal processing effect of vegetation spatial neighborhood density segmentation can be obtained when the neighborhood scale is taken as  $7 \times 7$ .

## ACKNOWLEDGEMENTS

This study was supported by the natural science foundation of Xinjiang Autonomous Region Project "Monitoring of urban leaf area index based on hyperspectral remote sensing images" (Grant No. 2021D01C054) and doctoral research startup fund project of Xinjiang University "Research on priority evaluation of multi-scale mine ecological restoration in Yili Valley" (Grant No. 202109120012). In addition, the constructive comments and suggestions from the handling editor and anonymous reviewers are gratefully acknowledged.

## REFERENCES

- [1]. Chen R X, Wang C F (2013) Review on Greenland recognition from urban high-resolution satellite imagery. *Remote Sensing Information*, 28(3): 119-125.
- [2]. Sotomayor A I T (2002) A spatial analysis of different forest cover types using GIS and remote sensing techniques.
- [3]. Riaño D, Chuvieco E, Salas J, et al. (2003) Assessment of different topographic corrections in Landsat-TM data for mapping vegetation types. *IEEE Transactions on geoscience and remote sensing*, 41(5): 1056-1061.
- [4]. Yesilnacar E, Süzen M (2006) A land-cover classification for landslide susceptibility mapping by using feature components. *International Journal of Remote Sensing*, 27(2): 253-275.
- [5]. Matsushita B, Yang W, Chen J, et al. (2007) Sensitivity of the enhanced vegetation index (EVI) and normalized difference vegetation index (NDVI) to topographic effects: a case study in high-density cypress forest. *Sensors*, 7(11): 2636-2651.
- [6]. Liu X, A Hou Z, Shi Z, et al. (2017) A shadow identification method using vegetation indices derived from hyperspectral data. *International Journal of Remote Sensing*, 38(19): 5357-5373.
- [7]. Jiang H, Jiang H, Wang S, et al. (2019) A shadow- eliminated vegetation index (SEVI) for removal of self and cast shadow effects on vegetation in rugged terrains. *International Journal of Digital Earth*, 12(9): 1013-1029.
- [8]. Xiao C, Xiao D, Zhang L, et al. (2013) Efficient shadow removal using subregion matching illumination transfer. *Computer Graphics Forum*, 32(7): 421-430.
- [9]. Pu Z, Yang L, Bai J (2008) Shadow detection and removal based on object-oriented method in high-resolution satellite imagery. *Remote Sensing Technology and Application*, 23(6): 735-738.
- [10]. Jiang H Y, Zhou J H (2013) Removing thin cloud cover from Remote Sensing images. *Remote Sensing Technology and Application*, 28(4): 640-646.
- [11]. Qin J, Leng H B, Zhao G Q, et al. (2017) Applications of phenology analysis and spectrum-location analysis in the classification of urban vegetation population. *Remote Sensing Technology and Application*, 32(5): 948-957.
- [12]. Foody G M. (2005) Local characterization of thematic classification accuracy through spatially constrained confusion matrices. *International Journal of Remote Sensing*, 26(6): 1217-1228.
- [13]. Comber A, Fisher P, Brunson C, et al. (2012) Spatial analysis of remote sensing image classification accuracy. *Remote Sensing of Environment*, 127: 237-246.
- [14]. Ok A O, Senaras C, Yuksel B (2013) Automated Detection of Arbitrarily Shaped Buildings in Complex Environments From Monocular VHR Optical Satellite Imagery. *IEEE Transactions on Geoscience and Remote*

Sensing, 51(3): 1701-1717.

- [15]. Sadeghi V, Farnood Ahmadi F, Ebadi H (2018) A new fuzzy measurement approach for automatic change detection using remotely sensed images. *Measurement*, 127: 1-14.
- [16]. Zhuang H, Fan H, Deng K, et al. (2018) A Spatial-Temporal Adaptive Neighborhood-Based Ratio Approach for Change Detection in SAR Images. *Remote Sensing*, 10(8): 1295.
- [17]. Melgani F, Moser G, Serpico S B (2002) Unsupervised change detection methods for remote-sensing images. *Opt Eng*, 41(12): 3288-3297.
- [18]. Niemeyer I, Marpu P R, Nussbaum S (2008) Change detection using object features. New York: Springer-Verlag.
- [19]. Carvalho Júnior O A, Guimarães R F, Gillespie A R, et al. (2011) A New Approach to Change Vector Analysis Using Distance and Similarity Measures. *Remote Sensing*, 3(11): 2473-2493.
- [20]. Chen J, Lu M, Chen X, et al. (2013) A spectral gradient difference based approach for land cover change detection. *ISPRS Journal of Photogrammetry and Remote Sensing*, 85: 1-12.